 

## *Headline Articles*

# Reaction Rate Spectroscopy for a Catalyzed Reaction of Gases

**Yusuke Yasuda,* Akira Matsumoto, and Ryo Oda**

Faculty of Science, Toyama University, Toyama 930-8555

Received March 10, 2004; E-mail: yasuda@sci.toyama-u.ac.jp

A "reaction rate spectroscopy" available for a catalyzed reaction of gases is proposed on the basis of a frequency response method by which the *flow* of Gibbs free energy along a reaction coordinate $\tau$, $J(\tau)$ ($\equiv [-\mathrm{d}G/\mathrm{d}t]_\tau$), can be determined. The validity was confirmed by actual data obtained in a reaction of $CO(g) + (1/2)O_2(g) \rightarrow CO_2(g)$ (I) on $Pt/Al_2O_3$, $Ru/Al_2O_3$, and Cu pellets at 623 K under partial pressures of ca. 100 Pa. The Gibbs free energy drop in the reaction (I), $-\Delta g_T$ ($> 0$), was found to be divided into two parts, $x(-\Delta g_T)$ and $y(-\Delta g_T)$ ($x + y = 1$), concerning the parallel transformations of the two reactants, (i) $CO(g) \rightarrow CO_2(g)$ and (ii) $(1/2)O_2(g) \rightarrow CO_2(g)$, respectively: $y = 0.158$ (on Pt), 0.124 (Ru), and 0.021 (Cu). Both transformations were assumed to occur via three elementary steps accompanied by two intermediates, A and B, represented by (i) $CO(X) \leftrightarrow CO(A_X) \leftrightarrow CO(B_X) \rightarrow CO_2(Z_X)$ and (ii) $(1/2)O_2(Y) \leftrightarrow (1/2)O_2(A_Y) \leftrightarrow O(B_Y) \rightarrow CO_2(Z_Y)$. Changes in $J(\tau)$ in the course of (i) and (ii), $\delta J_X(\tau_n)$ ($\equiv J_X(\tau_n) - J_X(\tau_{n-1})$) and $\delta J_Y(\tau_n)$, respectively, were determined along the reaction coordinate $\tau_n$ ($n = 1$–5; $n$ corresponds to the three steps and two intermediates). Although both $\delta J_X(\tau_n)$ and $\delta J_Y(\tau_n)$ were either negative or positive, the sum of $\delta J_X(\tau_n) + \delta J_Y(\tau_n)$ was negative throughout the reaction, in agreement with the second law of thermodynamics.

Catalysis is fundamentally a science of *kinetics*. In general, heterogeneous catalytic reactions represent systems far from thermodynamic equilibrium and therefore one can observe in such systems rate oscillations, spatiotemporal patterns, and chaos on a mesoscopic scale.[1,2] In far-from-equilibrium situations, we begin to observe new properties of matter which are hidden at equilibrium.[3] To know the kinetic nature from first principles seems to be very challenging. Although quantitative description of the complex phenomenon of catalysis is indispensable for this purpose, it is not easy.

Among heterogeneous catalytic reactions, a reaction of *gases* appears relatively simple. However, it is a series of at least three consecutive steps, i.e., adsorption, a surface reaction, and desorption illustrated by the mechanism shown in Fig. 1. In the steady state, however, because the rates of all consecutive steps are both constant and equal, a *stationary* measurement can give only a little information about the rates of individual steps. Under *nonstationary* conditions, there is no such constraint. It is believed that each step proceeds according to its own kinetic nature.[4–6]

Nonstationary methods have increasingly become the standard approach in the kinetic research of heterogeneous catalytic reactions. In transient methods, the reacting system is perturbed by a sudden or periodic change in temperature, pressure, flow rate, or composition. The response of the system is monitored by an appropriate analytical tool. Some frequency response (FR) techniques have been applied to study reaction kinetics in a gas/surface system.[7,8]

The basic principle of FR methods is that a system subjected

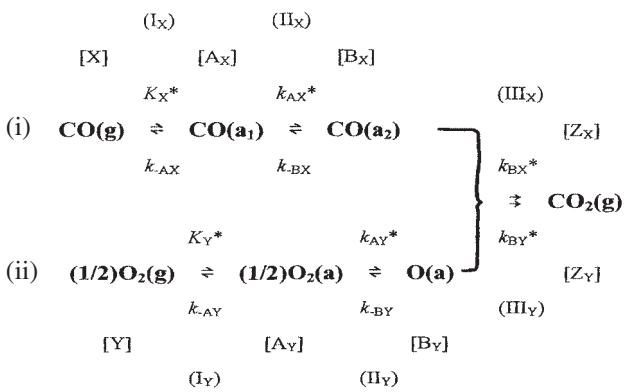


Fig. 1. Reaction mechanism for a CO oxidation reaction ($X + Y \rightarrow Z$) composed of the three elementary steps, I, II, and III, accompanied by the two intermediates, A and B. The whole reaction is divided into two parallel reactions, (i) $X \rightarrow A_X \rightarrow B_X \rightarrow Z_X$ and (ii) $Y \rightarrow A_Y \rightarrow B_Y \rightarrow Z_Y$. Every forward reaction ($\rightarrow$) is characterized by the complex rate coefficient $K^*$ ($\equiv K + i\omega L$) or $k^*$ ($\equiv k + i\omega l$), whereas every reverse reaction ($\leftarrow$) is characterized by real $k$.

to a periodic perturbation produces a periodic response that has a lower amplitude[9] and is shifted in phase with respect to the input. The frequency introduces an additional degree of freedom that can be used to decouple individual steps occurring with different characteristic relaxation times.[10,11] Since ampli-

Published on the web November 11, 2004; DOI 10.1246/bcsj.77.1973

tude changes and phase lags must be observed over several steady-state cycles, an open system of flow reactors is indispensable in keeping the steady state.

The FR techniques by means of a flow reactor can be divided into two types: (i) the gas space of a continuous-flow reactor is varied sinusoidally by a reciprocating piston, and the response is obtained from partial pressure variations of every reactant and product induced by the volume change, and (ii) the pressure at the inlet of a packed bed is varied by a synchronized mass flow controller or a reciprocating piston in a fluid stream, and the response is observed at the exit.

A mathematical and conceptual frame work for each FR method has been discussed by Yasuda[7] in the case of (i) and by Schrieffer and Sinfelt[8] in the case of (ii). The different techniques in order to produce sinusoidal variations in reactant concentrations in a flow reactor are essential in both the experimental and theoretical aspects, as shown below.

The FR method of type (i) was applied to a hydrogenation of propylene on supported Pt, a fairly simple and well-understood catalytic reaction. The shape of the response curves was reproducible only if a new type of pseudo-kinetic parameter was introduced, reflecting the response of hydrogenation rates to changes in the derivative of the dihydrogen pressure, an unusual and previously unreported effect in reaction kinetic treatments.[7]

To confirm the pseudo-kinetic parameter, a sophisticated reactor composed of a proton-conducting membrane was adopted.[12] It was found further that complex rate coefficients represented by $\{k + i\omega l\}$ are effective for forward reaction rates of elementary reactions.[13] After more detailed investigations, the imaginary part was correlated with free energy dissipations via surface intermediates.[14]

Recently,[15] the FR method has been applied to the best understood catalytic reaction of

$$\mathrm{CO(g)} + (1/2)\mathrm{O_2(g)} \rightarrow \mathrm{CO_2(g)};$$
$$-\Delta g_T{}^0 \text{ (or } -\Delta G_f{}^0) = 257.2 \text{ kJ} \quad (1)$$

because the reaction mechanism and kinetics are relatively simple compared with other catalytic processes.[16]

The reaction mechanism adopted is shown in Fig. 1, where parallel transformations of both reactant X and Y were assumed to occur via three steps accompanying two intermediates, A and B, represented by (i) $\mathrm{CO(X)} \leftrightarrow \mathrm{CO(A_X)} \leftrightarrow \mathrm{CO(B_X)} \leftrightarrow \mathrm{CO_2(Z_X)}$ and (ii) $(1/2)\mathrm{O_2(Y)} \leftrightarrow (1/2)\mathrm{O_2(A_Y)} \leftrightarrow \mathrm{O(B_Y)} \leftrightarrow \mathrm{CO_2(Z_Y)}$, where two kinds of adsorbed species of CO, $A_X$ and $B_X$, were assumed,[17] in accordance with the fact that both $CO_{ads}$ and $O_{ads}$ form separate domains at lower concentrations, while the further admission of CO leads to the formation of regions that form a mixed phase of $CO_{ads}$ and $O_{ads}$.[16] The reverse reaction in step III was confirmed to be negligibly small.[18]

On the basis of FR measurements carried out with some different catalysts, a "reaction rate spectroscopy (RRS)" is proposed in this work that is the first method to investigate the *flow* of Gibbs free energy along the reaction coordinate $\tau$, $[-\mathrm{d}G/\mathrm{d}t]_\tau$, which would be the heart of catalyzed reaction *rate*. The present method is therefore expected to play an essential role in studying heterogeneous catalysis.

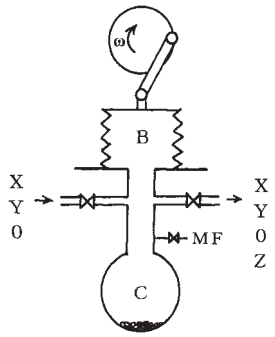


Fig. 2. Schematic diagram of RRS apparatus. A gas mixture of the reactants, X and Y, and 0 as a reference gas, is admitted to the constant-flow reactor; the mixture involving the product Z is evacuated from the other side. (C) catalysts; (B) bellows to vary the gas space; (MF) mass spectrometer.

Table 1. Experimental Conditions (Units of Pressure: Pa)

| $P_{total}$ | $P_X{}^{(s)}$ | $P_Y{}^{(s)}$ | $P_Z{}^{(s)}$ | $P_Z{}^{(s)}$ | $\sigma$/min$^{-1}$ |
|---|---|---|---|---|---|
| 365 | 116 | 86 | 72 | 91 | 0.60 |
| 377 | 120 | 90 | 74 | 93 | 0.56 |
| 368 | 119 | 88 | 72 | 89 | 0.56 |

## 1. Experimental

The apparatus for RRS is schematically shown in Fig. 2, the details of which were described previously.[15] A gas mixture of CO(X), $O_2$(Y), and Ar(0) as a reference standard was admitted to the flow reactor at a constant supply rate. The partial pressure of each component in the reactor was ca. 100 Pa in the steady state. Reaction conditions are summarized in Table 1.

Three kinds of catalysts were adopted in this work: 0.5 wt % $Pt/Al_2O_3$ (1.6 g; reference catalyst of JRC-A4-0.5Pt, The Catalysis Society of Japan), 0.5 wt % $Ru/Al_2O_3$ (1.8 g; reference catalyst of JRC-A4-0.5Ru), and commercial Cu pellets (14.2 g) for gravimetric analysis. They were evacuated for at least half an hour at 623 K, and the flow of the gas mixture was kept at the same temperature for at least half an hour before FR measurements.

The gas space of the flow reactor was varied sinusoidally. The variation was expressed well (using complex notation) by

$$V(t) = V_0 + \Delta V(t);\ \Delta V(t)/V_0 \equiv -v\exp(i\omega t) \quad (2)$$

where $V_0$ (= ca. 1 dm$^3$) denotes the mean volume, $v$ (= ca. $10^{-2}$) is the relative amplitude of the variation, and $\omega$ is the angular frequency of the harmonic oscillation.

The partial-pressure variation of component W, $P_W(t)$ (W = X, Y, Z, or 0), was expressed well by

$$P_W(t) = P_W{}^{(s)} + \Delta P_W(t);\ \Delta P_W(t)/P_W{}^{(s)} \equiv p_W{}^*\exp(i\omega t);\ p_W{}^* \equiv p_W\exp(i\phi_W) \quad (3)$$

where $P_W{}^{(s)}$ denotes the partial pressure in the steady state, $p_W$ is the relative amplitude of the oscillation, and $\phi_W$ is the phase difference between the volume and pressure variations. Each pressure variation was followed by a quadrupole mass spectrometer analysis, and ($p_W$, $\phi_W$) were observed at a definite $\omega$. $\omega$ was scanned over a wide range.

After a run of one component (i.e., X, Y, Z, or 0) scanned over a wide range of $\omega$, the run of another component was followed under almost the same conditions.

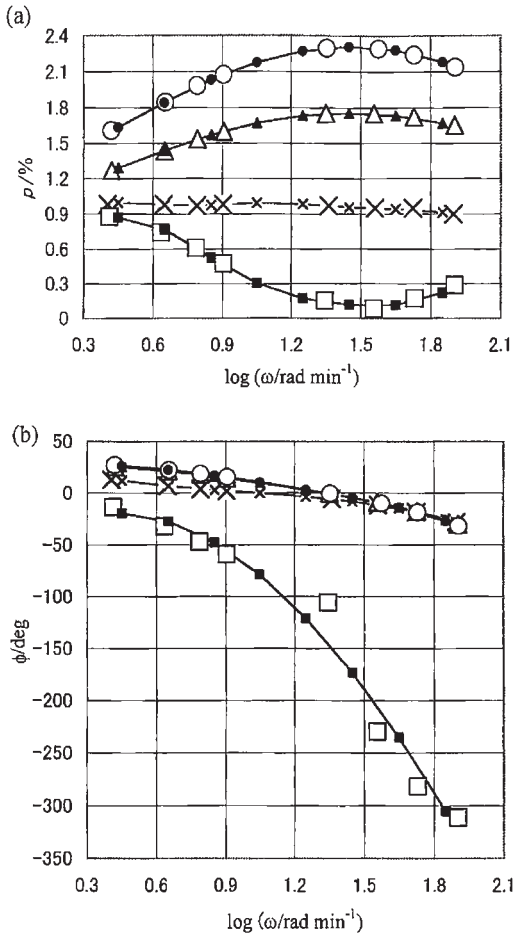


Fig. 3. FR data obtained by Pt catalyst at 623 K. (a) Relative amplitude of each partial-pressure variation, $p_W$, versus the angular frequency $\omega$ (W = X, Y, Z, and 0). (b) Phase difference between each partial-pressure and volume variations, $\phi_W$, versus $\omega$. (△) that of CO(g); (○) that of $O_2$(g); (□) that of $CO_2$(g); (×) that of Ar(g). (▲), (●), (■), and (×) represent those interpolated to the definite eight $\omega$'s using the smoothed curves.

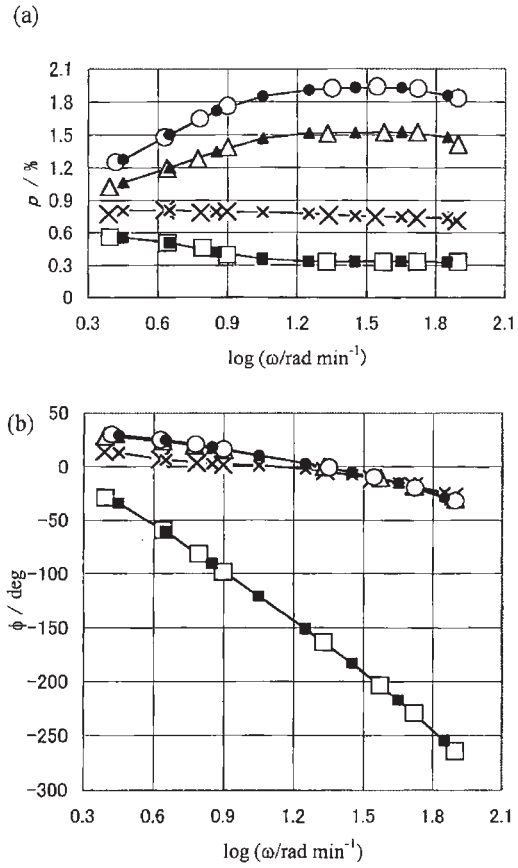


Fig. 4. FR data obtained by Ru catalyst at 623 K. Notation is that of Fig. 3.

## 2. Frequency Response Data

Actual FR data on ($p_W$, $\phi_W$) obtained by the three kinds of catalysts are plotted versus $\omega$ in Figs. 3–5. It is worth noting that (i) the relative amplitude of the reactants are larger[9] than that of Ar, which has never been observed in an adsorption/desorption system, and (ii) the phase lags of reactants and that of the product are on the opposite sides of Ar.

These raw data were interpolated to common eight $\omega_j$'s using polynomials in $\log(\omega_j/\text{radians min}^{-1})$: $\omega_1 = 10^{0.45}$, $\omega_2 = 10^{0.65}$, $\omega_3 = 10^{0.85}$, $\omega_4 = 10^{1.05}$, $\omega_5 = 10^{1.25}$, $\omega_6 = 10^{1.45}$, $\omega_7 = 10^{1.65}$, and $\omega_8 = 10^{1.85}$ in order to compare them with each other.

The data on ($p_W$, $\phi_W$) interpolated to the definite $\omega_j$'s were transformed to

$$(p_W/p_0)\cos(\phi_W - \phi_0) - 1 \equiv f_{cW}{}^{(exp)}(\omega) \quad (4)$$

$$(p_W/p_0)\sin(\phi_W - \phi_0) \equiv f_{sW}{}^{(exp)}(\omega) \quad (5)$$

because these are suitable to compare the experimental results with the theoretical ones derived from the reaction mechanism. It is worth noting that only the ratio ($p_W/p_0$) and the difference ($\phi_W - \phi_0$) with respect to the reference gas were used in Eqs. 4 and 5, and therefore any apparent change due to the apparatus would be removed.

The in-phase and out-of-phase components of Eqs. 4 and 5, respectively, are plotted on the $x$- and $y$-axis in Figs. 6(a)–8(a). Since the origin (0, 0) corresponds to those of Ar, which is inert in the reaction, the deviation from the origin may be attributed to the reaction *rate*. It is worth noting that the plots for the *disappearance* rates of X and Y and those for the *appearance* rate of Z were on the opposite sides of (0, 0).

## 3. FR Data Analysis

Theoretical formulas corresponding to $f_{cW}{}^{(exp)}(\omega)$ and $f_{sW}{}^{(exp)}(\omega)$ in Eqs. 4 and 5 can be derived from the reaction mechanism as described below.

**3.1 Expressions for $\Delta A(t)$ and $\Delta B(t)$ in Terms of $\Delta P(t)$.** When the partial pressure of the reactants are perturbed, the amounts of every intermediate are also varied. Although the variations of intermediate $\Delta A_X(t)$, $\Delta B_X(t)$, $\Delta A_Y(t)$, and $\Delta B_Y(t)$ cannot be directly observed, they can be expressed in terms of $\Delta P_X(t)$ and $\Delta P_Y(t)$ on the basis of material balance.

The appearance rate of $B_X$, $dB_X/dt$, for example, may be described (irrespective of any non-linear rate equation) by[19]

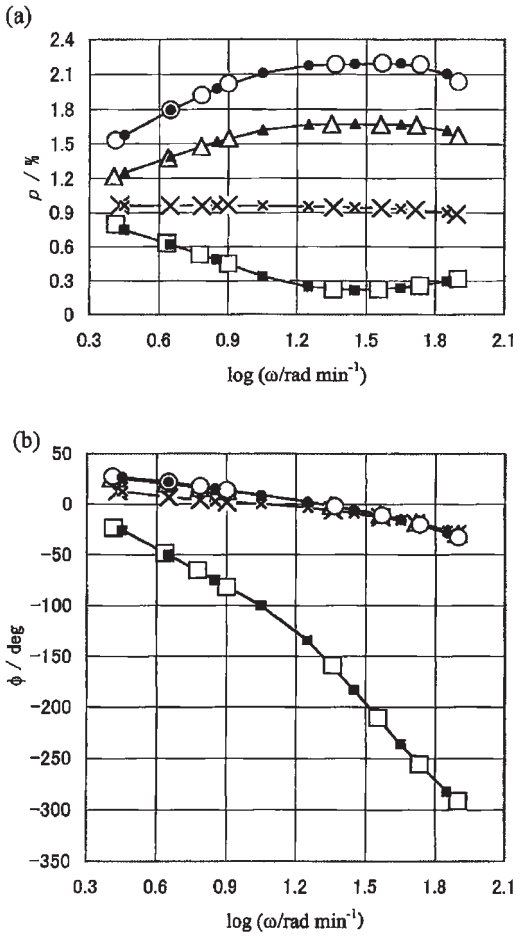


Fig. 5. FR data obtained by Cu catalyst at 623 K. Notation is that of Fig. 3.

$$\mathrm{d}B_X(t)/\mathrm{d}t = k_{AX}{}^{*}\Delta A_X(t) - k_{-BX}\Delta B_X(t) - k_{BX}{}^{*}\Delta B_X(t) - k_{BY}{}^{*}\Delta B_Y(t) \quad (6)$$

where $k_{AX}{}^{*}$, for example, means the complex rate coefficient defined by $k_{AX} + i\omega l_{AX}$. Every rate coefficient for the forward reaction at every elementary step is assumed to be complex according to the results reported in Ref. 14. It is worth noting that the last term $k_{BY}{}^{*}\Delta B_Y(t)$ arises from the binding of $B_X$ with $B_Y$ (= O(a)) in the last step of $III_X$, which leads to coupling among terms concerned with X-, Y-, and Z-components.

On the other hand, the left hand side can be replaced by $i\omega\Delta B_X(t)$ because $\Delta B_X(t)$ varies harmonically. Consequently, Eq. 6 can be rewritten as

$$-k_{AX}{}^{*}\Delta A_X(t) + (k_{-BX} + k_{BX}{}^{*} + i\omega)\Delta B_X(t) + k_{BY}{}^{*}\Delta B_Y(t) = 0. \quad (7)$$

According to a similar procedure for the rates of other intermediates, the material balances concerning $\mathrm{d}A_X(t)/\mathrm{d}t$, $\mathrm{d}A_Y(t)/\mathrm{d}t$, and $\mathrm{d}B_Y(t)/\mathrm{d}t$ lead to

$$(k_{-AX} + k_{AX}{}^{*} + i\omega)\Delta A_X(t) - k_{-BX}\Delta B_X(t) = K_X{}^{*}\Delta P_X(t) \quad (8)$$

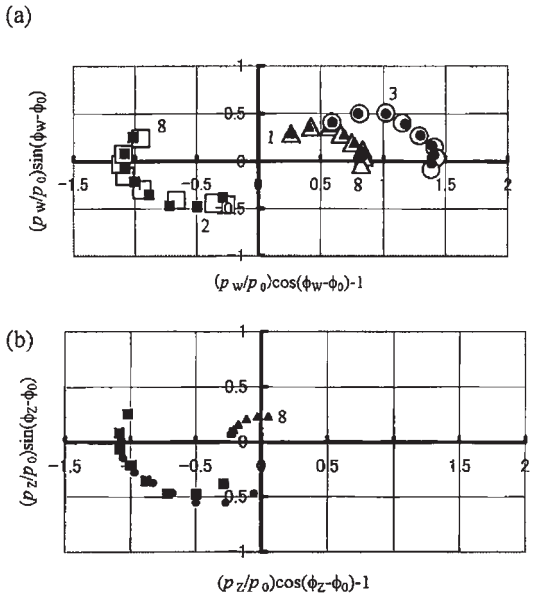


Fig. 6. RRS by Pt catalyst derived from the FR data shown in Fig. 3. (a) Comparison of $[f_{cW}{}^{(exp)}(\omega), f_{sW}{}^{(exp)}(\omega)]$ represented by the open symbols with $[f_{cW}{}^{(calc)}(\omega)$ and $f_{sW}{}^{(calc)}(\omega)]$ represented by the solid symbols (W = X, Y, and Z). (△) that of CO(g); (○) that of $O_2$(g); (□) that of $CO_2$(g). (▲), (●), and (■) represent those calculated using sixteen parameters summarized in Table 2. (b) Contribution of $\Delta P_X(t)$ (▲) and $\Delta P_Y(t)$ (●) to $\Delta R(t)$ (■) derived from Eq. 34; (▲) and (●) represent the first and second terms on the right hand side of Eq. 34, respectively; (■), the calculated results by Eq. 34 that are the same as those plotted in (a). The number indicates the value of $\log(\omega/\mathrm{rad\,min^{-1}})$: **1** (= 0.45), **2** (= 0.65), **3** (= 0.85), **4** (= 1.05), **5** (= 1.25), **6** (= 1.45), **7** (= 1.65), and **8** (= 1.85).

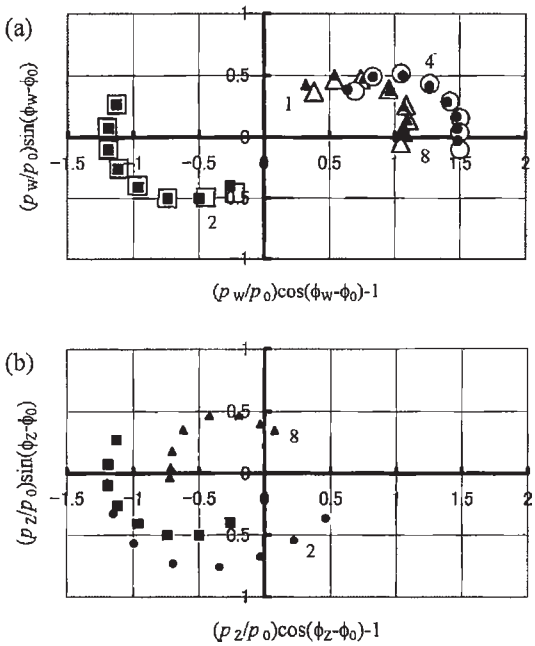


Fig. 7. RRS by Ru catalyst derived from the FR data shown in Fig. 4. Notation is that of Fig. 6.

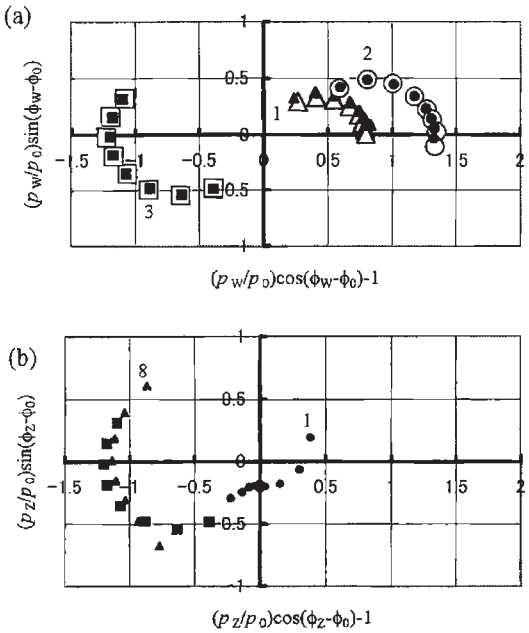


Fig. 8. RRS by Cu catalyst derived from the FR data shown in Fig. 5. Notation is that of Fig. 6.

$$(k_{-AY} + k_{AY}^* + i\omega)\Delta A_Y(t) - k_{-BY}\Delta B_Y(t) = K_Y^*\Delta P_Y(t) \quad (9)$$

$$-k_{AY}^*\Delta A_Y(t) + (k_{-BY} + k_{BY}^* + i\omega)\Delta B_Y(t) + k_{BX}^*\Delta B_X(t) = 0 \quad (10)$$

respectively.

Since these four simultaneous equations are linear in form, Eqs. 7–10 can be easily solved, and we have the solutions:

$$\Delta A_X(t) = \{K_X^*/(k_{-AX} + k_{AX}^* + i\omega)\}\{1 + k_{AX}^*k_{-BX}\Theta_Y/\Gamma\}\Delta P_X(t) - \{K_Y^*k_{AY}^*k_{BY}^*k_{-BX}/\Gamma\}\Delta P_Y(t) \quad (11)$$

$$\Delta A_Y(t) = -\{K_X^*k_{AX}^*k_{BX}^*k_{-BY}/\Gamma\}\Delta P_X(t) + \{K_Y^*/(k_{-AY} + k_{AY}^* + i\omega)\}\{1 + k_{AY}^*k_{-BY}\Theta_X/\Gamma\}\Delta P_Y(t) \quad (12)$$

$$\Delta B_X(t) = (K_X^*k_{AX}^*\Theta_Y/\Gamma)\Delta P_X(t) - \{K_Y^*k_{AY}^*k_{BY}^*(k_{-AX} + k_{AX}^* + i\omega)/\Gamma\}\Delta P_Y(t) \quad (13)$$

$$\Delta B_Y(t) = -\{K_X^*k_{AX}^*k_{BX}^*(k_{-AY} + k_{AY}^* + i\omega)/\Gamma\}\Delta P_X(t) + (K_Y^*k_{AY}^*\Theta_X/\Gamma)\Delta P_Y(t) \quad (14)$$

where the following abbreviation

$$\Theta_X \equiv (k_{-AX} + k_{AX}^* + i\omega)(k_{-BX} + k_{BX}^* + i\omega) - k_{AX}^*k_{-BX} \quad (15)$$

$$\Theta_Y \equiv (k_{-AY} + k_{AY}^* + i\omega)(k_{-BY} + k_{BY}^* + i\omega) - k_{AY}^*k_{-BY} \quad (16)$$

and

$$\Gamma \equiv \Theta_X\Theta_Y - (k_{-AX} + k_{AX}^* + i\omega)(k_{-AY} + k_{AY}^* + i\omega)k_{BX}^*k_{BY}^* \quad (17)$$

has been introduced.

**3.2 Theoretical Formulas of $f_{cW}^{(calc)}(\omega)$ and $f_{sW}^{(calc)}(\omega)$.** On the basis of material balances with respect to the components of X, Y, Z, and 0 in the gas phase, we can derive $f_{cW}^{(calc)}(\omega)$ and $f_{sW}^{(calc)}(\omega)$ as follows:

(1) Since the partial pressure of every component was low enough (ca. 100 Pa), the composition of the gas mixture in the reactor may be regarded as spatially uniform, as confirmed previously.[7] Therefore, material balance with respect to X leads to

$$dX(t)/dt = F_X - R_s - K_X^*\Delta P_X(t) + k_{-AX}\Delta A_X(t) - \sigma'\{P_X^{(s)} + \Delta P_X(t)\} \quad (18)$$

where $F_X$ denotes the constant feed of gaseous CO, $R_s$ is the overall reaction rate at the steady state, and the disappearance rate through the exit can be expressed in term of constant $\sigma'$ corresponding to the size of orifice by $\sigma' P_X(t)$, because the outside was evacuated and therefore the pressure gap at the orifice is $P_X(t)$. On the other hand, since every gas may be regarded as ideal, $X(t)$ can be given by

$$X(t) = P_X(t)V(t)/(RT_0). \quad (19)$$

Substituting Eqs. 2 and 3 into Eq. 19, we have

$$\Delta X(t) = (P_X^{(s)}V_0/RT_0)(p_X^* - v)\exp(i\omega t). \quad (20)$$

Substituting Eq. 20 and Eq. 11 describing $\Delta A_X(t)$ into Eq. 18, we have (after some rearrangements)

$$(\sigma + i\omega)p_X^* - i\omega v = k_X^*\{k_{-AX}(1 + k_{AX}^*k_{-BX}\Theta_Y/\Gamma)/(k_{-AX} + k_{AX}^* + i\omega) - 1\}p_x^* - (P_Y^{(s)}/P_X^{(s)})(k_Y^*k_{AY}^*k_{BY}^*k_{-AX}k_{-BX}/\Gamma)p_Y^* \quad (21)$$

where the short notation

$$k_X^* \equiv (RT_0/V_0)K_X^*;\ k_Y^* \equiv (RT_0/V_0)K_Y^*;\ \sigma \equiv (RT_0/V_0)\sigma' \quad (22)$$

has been introduced.

Because the reaction mechanism of Y is the same in form as that of X (see Fig. 1), the results for the Y-component can be easily derived from Eq. 21 by replacing X for Y and vice versa:

$$(\sigma + i\omega)p_Y^* - i\omega v = k_Y^*\{k_{-AY}(1 + k_{AY}^*k_{-BY}\Theta_X/\Gamma)/(k_{-AY} + k_{AY}^* + i\omega) - 1\}p_y^* - (P_X^{(s)}/P_Y^{(s)})(k_X^*k_{AX}^*k_{BX}^*k_{-AY}k_{-BY}/\Gamma)p_X^*. \quad (23)$$

According to a similar procedure for $dZ(t)/dt$, we have

$$dZ(t)/dt = R_s + k_{BX}^*\Delta B_X(t) + k_{BY}^*\Delta B_Y(t) - \sigma'\{P_Z^{(s)} + \Delta P_Z(t)\}. \quad (24)$$

Substituting expressions for $\Delta B_X(t)$ and $\Delta B_Y(t)$ given in Eqs. 13 and 14, respectively, into Eq. 24, we have (after some rearrangements)

$$(\sigma + i\omega)p_Z^* - i\omega v = [(P_X^{(s)}/P_Z^{(s)})k_X^* k_{AX}^* k_{BX}^* \{\Theta_Y - (k_{-AY} + k_{AY}^* + i\omega)k_{BY}^*\}/\Gamma]p_X^* + [(P_Y^{(s)}/P_Z^{(s)})k_Y^* k_{AY}^* k_{BY}^* \{\Theta_X - (k_{-AX} + k_{AX}^* + i\omega)k_{BX}^*\}/\Gamma]p_Y^*. \quad (25)$$

On the other hand, a similar treatment for Ar leads to

$$(\sigma + i\omega)p_0^* - i\omega v = 0 \text{ or } (\sigma + i\omega)p_0^* = i\omega v \quad (26)$$

because every rate coefficient may be regarded as zero in the case of inert gas and therefore every term on the right hand side of Eqs. 21, 23, or 25 disappears.

(2) Combining Eqs. 21 and 26, we have

$$(p_X^*/p_0^*) - 1 = [k_X^*\{k_{-AX}(1 + k_{AX}^* k_{-BX}\Theta_Y/\Gamma)/(k_{-AX} + k_{AX}^* + i\omega) - 1\}(p_X^*/p_0^*) - (P_Y^{(s)}/P_X^{(s)})(k_Y^* k_{AY}^* k_{BY}^* k_{-AX}k_{-BX}/\Gamma)(p_Y^*/p_0^*)]/(\sigma + i\omega). \quad (27)$$

Since the ratio $(p_X^*/p_0^*)$ can be rewritten as $(p_X/p_0)\exp\{i(\phi_X - \phi_0)\}$, the real and imaginary parts on the left hand side of Eq. 27 correspond to Eqs. 4 and 5, respectively, so that we have

$$f_{cX}^{(calc)}(\omega) + if_{sX}^{(calc)}(\omega) = \{H_{XX}^*(\omega)(p_X^*/p_0^*) + H_{XY}^*(\omega)(P_Y^{(s)}/P_X^{(s)})(p_Y^*/p_0^*)\}/(\sigma + i\omega) \quad (28)$$

where

$$H_{XX}^*(\omega) = k_X^*\{k_{-AX}(1 + k_{AX}^* k_{-BX}\Theta_Y/\Gamma)/(k_{-AX} + k_{AX}^* + i\omega) - 1\} \quad (29)$$

$$H_{XY}^*(\omega) = -k_Y^* k_{AY}^* k_{BY}^* k_{-AX}k_{-BX}/\Gamma. \quad (30)$$

Comparing real and imaginary parts on both sides of Eq. 28, we have the final results for theoretical expressions:

$$f_{cX}^{(calc)}(\omega) = \mathrm{Re}[\{H_{XX}^*(\omega)(p_X^*/p_0^*) + H_{XY}^*(\omega)(P_Y^{(s)}/P_X^{(s)})(p_Y^*/p_0^*)\}/(\sigma + i\omega)] \quad (31)$$

$$f_{sX}^{(calc)}(\omega) = \mathrm{Im}[\{H_{XX}^*(\omega)(p_X^*/p_0^*) + H_{XY}^*(\omega)(P_Y^{(s)}/P_X^{(s)})(p_Y^*/p_0^*)\}/(\sigma + i\omega)]. \quad (32)$$

In a similar way, Eqs. 23 and 25 lead to

$$f_{cY}^{(calc)}(\omega) + if_{sY}^{(calc)}(\omega) = \{H_{YX}^*(\omega)(P_X^{(s)}/P_Y^{(s)})(p_X^*/p_0^*) + H_{YY}^*(\omega)(p_Y^*/p_0^*)\}/(\sigma + i\omega) \quad (33)$$

and

$$f_{cZ}^{(calc)}(\omega) + if_{sZ}^{(calc)}(\omega) = \{H_{ZX}^*(\omega)(P_X^{(s)}/P_Z^{(s)})(p_X^*/p_0^*) + H_{ZY}^*(\omega)(P_Y^{(s)}/P_Z^{(s)})(p_Y^*/p_0^*)\}/(\sigma + i\omega) \quad (34)$$

respectively, where

$$H_{YX}^*(\omega) = -k_X^* k_{AX}^* k_{BX}^* k_{-AY}k_{-BY}/\Gamma \quad (35)$$

$$H_{YY}^*(\omega) = k_Y^*\{k_{-AY}(1 + k_{AY}^* k_{-BY}\Theta_X/\Gamma)/(k_{-AY} + k_{AY}^* + i\omega) - 1\} \quad (36)$$

$$H_{ZX}^*(\omega) = k_X^* k_{AX}^* k_{BX}^* \{\Theta_Y - (k_{-AY} + k_{AY}^* + i\omega)k_{BY}^*\}/\Gamma \quad (37)$$

$$H_{ZY}^*(\omega) = k_Y^* k_{AY}^* k_{BY}^* \{\Theta_X - (k_{-AX} + k_{AX}^* + i\omega)k_{BX}^*\}/\Gamma. \quad (38)$$

Comparing real and imaginary parts on both sides of Eqs. 33 and 34, we can explicitly derive the formulas for $[f_{cY}^{(calc)}(\omega), f_{sY}^{(calc)}(\omega)]$ and $[f_{cZ}^{(calc)}(\omega), f_{sZ}^{(calc)}(\omega)]$.

**3.3 Evaluation of $\sigma$.** Equation 26 leads to

$$\phi_0(\omega) = \tan^{-1}(\sigma/\omega) \quad (39)$$

$$p_0(\omega)/v = \omega/(\sigma^2 + \omega^2)^{1/2}. \quad (40)$$

Comparing Eqs. 39 and/or 40 with actual data, we can determine the value of $\sigma$.[15] The results are given in Table 1.

**3.4 Determination of Rate Coefficients.** Comparing $[f_{cW}^{(exp)}(\omega), f_{sW}^{(exp)}(\omega)]$ with $[f_{cW}^{(calc)}(\omega), f_{sW}^{(calc)}(\omega)]$ (W = X, Y, and Z), we can determine all (sixteen) rate coefficients involved in the reaction mechanism of Fig. 1. In the numerical simulation, the term $(p_W^*/p_0^*)$ on the right hand sides of Eqs. 28, 33, and 34 was replaced by empirical results, and the rate coefficients were determined on a trial and error basis using a personal computer.

The calculated results are compared with experimental ones in Figs. 6(a)–8(a). The kinetic parameters[20] in Table 2 were used to derive the calculated results represented by the solid symbols. Evidently, a wider range of $\omega$ scanned is desirable to determine more reliable parameters.

The first and second terms on the right hand side of Eq. 34 are attributable to $\Delta P_X(t)$ and $\Delta P_Y(t)$, respectively. Therefore, the contribution of $\Delta P_X(t)$ and $\Delta P_Y(t)$ to the variation of the appearance rate of $CO_2$, $\Delta R(t)$, can be determined individually. These are shown in Figs. 6(b)–8(b).

It should be emphasized that only if *complex* rate coefficients have been employed in the reaction mechanism, will the FR data be reproduced well. The imaginary part, $i\omega l$, is not required by traditional methods of stationary measurement because $\omega = 0$. The imaginary part of $l$ plays an essential role in RRS, as discussed below.

## 4. New Concept of *J*

**4.1 Free Energy Dissipation via an Intermediate.** (1) Let us introduce free energy dissipation $w_{AX}$ and $w_{BX}$ via the $A_X$- and $B_X$-species (or $w_{AY}$ and $w_{BY}$ via the $A_Y$- and $B_Y$-species), respectively, illustrated by zigzag lines in Fig. 9. $\alpha_I$, $\alpha_{II}$, and $\alpha_{III}$ denote the affinities[3] of the reactions at I-, II-, and III-steps, respectively, where X or Y is omitted for simplicity.

Because the reaction mechanisms for X and Y are the same in form (see Fig. 1), the following results concerned with X can be easily transformed to those of Y by replacing X for Y.

The "free energy balance" involving the dissipations may be described by the difference between the increasing and decreasing free energies:

$$A_X^{(s)}w_{AX}^{(s)} = \alpha_{IX}R_s - \alpha_{IIX}R_s \quad (41)$$

$$B_X^{(s)}w_{BX}^{(s)} = \alpha_{IIX}R_s - \alpha_{IIIX}R_s \quad (42)$$

where $R_s$ may be given by $\sigma' P_Z^{(s)}$ (see Eq. 24). The affinities

Table 2. Rate Coefficient of the Reaction Mechanism Shown in Fig. 1 Determined by Numerical Simulation (Units of $k$: $min^{-1}$)

| Catal. | $k_X$[a)] | $l_X$[a)] | $k_{-AX}$ | $k_{AX}$ | $l_{AX}$ | $k_{-BX}$ | $k_{BX}$ | $l_{BX}$ | $k_Y$[b)] | $l_Y$[b)] | $k_{-AY}$ | $k_{AY}$ | $l_{AY}$ | $k_{-BY}$ | $k_{BY}$ | $l_{BY}$ | dev[c)] |
|---|---|---|---|---|---|---|---|---|---|---|---|---|---|---|---|---|---|
| Pt | −1.512 | −0.520 | 28.1 | 15.4 | −0.333 | 294 | 81.2 | 0.904 | −0.730 | −0.582 | 1.15 | 0.435 | −0.495 | −0.074 | 0.280 | −0.505 | 3.70 |
| Ru | −0.787 | −0.555 | 9.6 | 23.5 | −0.333 | 132 | 36.0 | 0.501 | −0.656 | −0.593 | 1.01 | 1.22 | −0.497 | −0.91 | 1.15 | −0.503 | 1.81 |
| Cu | 0.213 | −0.536 | 31.0 | 134 | −0.333 | 1885 | 1585 | 0.050 | 0.034 | −0.568 | 0.44 | 3.98 | −0.488 | −2.89 | 2.09 | −0.512 | 1.84 |

a) $k_X \equiv (RT_0/V_0)K_X$, $l_X \equiv (RT_0/V_0)L_X$. b) $k_Y \equiv (RT_0/V_0)K_Y$, $l_Y \equiv (RT_0/V_0)L_Y$. c) $\text{dev} \equiv (1/N)\Sigma_N[\{(\text{obs}_X - \text{calc}_X)^2\}^{1/2}/(\text{obs}_X)_{MAX} + \{(\text{obs}_Y - \text{calc}_Y)^2\}^{1/2}/(\text{obs}_Y)_{MAX} + \{(\text{obs}_Z - \text{calc}_Z)^2\}^{1/2}/(\text{obs}_Z)_{MAX}] \times (1/3) \times 100$.

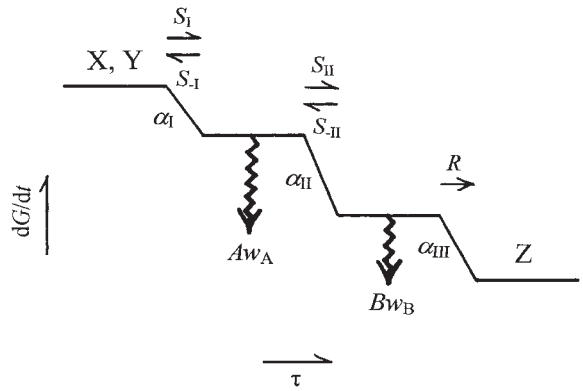


Fig. 9. Flow of Gibbs free energy along a reaction coordinate $\tau$. $\alpha_I$, $\alpha_{II}$, and $\alpha_{III}$: the affinities of the reactions at the elementary step I, II, and III. $S_I$ and $S_{II}$: the forward reaction rates at I- and II-steps. $S_{-I}$ and $S_{-II}$: the reverse reaction rates at I- and II-steps. $R$: the appearance rate of $CO_2$. $Aw_A$ and $Bw_B$: the free energy dissipations to maintain free energy balances.

are given by $\alpha_{IX} = \mu_X - \mu_{AX}$, $\alpha_{IIX} = \mu_{AX} - \mu_{BX}$, and $\alpha_{IIIX} = \mu_{BX} - \mu_{ZX}$ in terms of chemical potentials. $\mu_X$ and $\mu_{AX}$, for example, denote the chemical potentials of X- and $A_X$-species, respectively.

(2) Equations 41 and 42 in the steady state can be extended (in a non-steady state) to

$$A_X w_{AX} = \alpha_{IX}(S_{IX} - S_{-IX}) - \alpha_{IIX}(S_{IIX} - S_{-IIX}) \quad (43)$$

$$B_X w_{BX} = \alpha_{IIX}(S_{IIX} - S_{-IIX}) - \alpha_{IIIX} R \quad (44)$$

where $S_{IX}$ and $S_{IIX}$ denote the forward reaction rates at $I_X$- and $II_X$-steps, $S_{-IX}$ and $S_{-IIX}$ denote the reverse reaction rates at $I_X$- and $II_X$-steps, and $R$ is the appearance rate of $CO_2$ at the last step.

Let us consider variations of all terms in Eqs. 43 and 44 induced by $\Delta P_X(t)$. Considering $\Delta(A_X w_{AX})$, $\Delta(S_{IX} - S_{-IX})$, $\Delta(S_{IIX} - S_{-IIX})$, $\Delta(B_X w_{BX})$, $\Delta(S_{IIX} - S_{-IIX})$, and $\Delta R$, we have (after some rearrangements)[13]

$$\Delta w_{AX} = \{\alpha_{IX} + l_{AX}(\alpha_{IX} - \alpha_{IIX})\}(d\Delta A_X(t)/dt)/A_X^{(s)} \quad (45)$$

$$\Delta w_{BX} = \{\alpha_{IIX} + l_{BX}(\alpha_{IIX} - \alpha_{IIIX})\}(d\Delta B_X(t)/dt)/B_X^{(s)}. \quad (46)$$

However, $\Delta w_{AX}$ and $\Delta w_{BX}$ are expected not to depend on the perturbation, because $w_{AX}$ and $w_{BX}$ are intensive variables. Since both $d\Delta A_X(t)/dt$ and $d\Delta B_X(t)/dt$ are not zero, the theoretical expectation is satisfied only if

$$\alpha_{IX} + l_{AX}(\alpha_{IX} - \alpha_{IIX}) = 0 \quad (47)$$

$$\alpha_{IIX} + l_{BX}(\alpha_{IIX} - \alpha_{IIIX}) = 0. \quad (48)$$

On the other hand, the definition of every affinity leads to

$$\alpha_{IX} + \alpha_{IIX} + \alpha_{IIIX} = \mu_X - \mu_{ZX} \ (\equiv x(-\Delta g_T)) \quad (49)$$

where $-\Delta g_T$ ($> 0$) denotes the Gibbs free energy drop in the reaction of Eq. 1. The value of $x$ defined in Eq. 49 is the contribution of free energy drop in the transformation of (i) in Fig. 1 to that of $(-\Delta g_T)$.

Solving the simultaneous equations of Eqs. 47–49, we have expressions for every affinity in terms of $l$:

$$\alpha_{IX} = (l_{AX}l_{BX}/L_X)x(-\Delta g_T) \quad (50)$$

$$\alpha_{IIX} = \{(1 + l_{AX})l_{BX}/L_X\}x(-\Delta g_T) \quad (51)$$

$$\alpha_{IIIX} = \{(1 + l_{AX})(1 + l_{BX})/L_X\}x(-\Delta g_T) \quad (52)$$

where the abbreviation

$$L_X \equiv 1 + l_{AX} + 2l_{BX} + 3l_{AX}l_{BX} \quad (53)$$

has been introduced.

Substituting Eqs. 50–52 into Eqs. 41 and 42, we have expressions for the free energy dissipations:

$$A_X{}^{(s)}w_{AX}{}^{(s)} = -(l_{BX}/L_X)x(-\Delta g_T)R_s \quad (54)$$

$$B_X{}^{(s)}w_{BX}{}^{(s)} = -\{(1 + l_{AX})/L_X\}x(-\Delta g_T)R_s. \quad (55)$$

The sum of Eqs. 54 and 55 leads to

$$A_X{}^{(s)}w_{AX}{}^{(s)} + B_X{}^{(s)}w_{BX}{}^{(s)} = -\{(1 + l_{AX} + l_{BX})/L_X\}x(-\Delta g_T)R_s. \quad (56)$$

It should be emphasized that Eqs. 50–52 and also Eqs. 54–56 were deduced from the "free-energy balance" assumed in Eqs. 41 and 42.

**4.2 Definition of $\delta J(\tau)$.** If the feed of the reactant $F_X$ in Eq. 18 was stopped abruptly, the Gibbs free energy of the system would necessarily decay along the slant line as illustrated in Fig. 10(a), where $t_L$ is the elapsed time of the reaction, while the continuous supply of the reactant would keep the steady state of $(-\Delta g_T)R_s$, which is represented by the vertical line at $t = 0$. The steady state is perturbed by the entrance of catalysts as $\Delta P_X(t)$ and $\Delta P_Y(t)$ oscillating harmonically with $\omega$. The effect of the perturbation would depend on $\omega$. The slower, the deeper and vice versa as demonstrated in Fig. 10(b).

(1) Let us introduce $J(\tau)$ given by

$$J(\tau)\ (\equiv [-dG/dt]_\tau) = -[(d\mu/dt)N + \mu(dN/dt)]_\tau \quad (57)$$

where $G$ is replaced by $\mu N$. The change $\delta J(\tau_n)$ via each elementary process is defined as

$$\delta J(\tau_n) \equiv J(\tau_n) - J(\tau_{n-1});\ \tau_n \equiv n\delta\tau \quad (58)$$

where the reaction coordinate $\tau_n$ ($n = 1$–5) is defined by constant $\delta\tau$, demonstrated in Fig. 10(b). It should be emphasized that the five elementary processes are separated by the identical $\delta\tau$.[21]

(2) The change $\delta J(\tau_n)$ along $\tau_n$ concerning the X-component can be derived as follows.

(i) In the first step, $I_X$, the term $(d\mu/dt)$ in Eq. 57 may be regarded as zero, because $\mu$ does not depend on $t$ at $I_X$, so that we have

$$J_X(\tau) = -\{0 + \mu(dN/dt)\}_\tau;\ \tau_0 \leqq \tau \leqq \tau_1. \quad (59)$$

The change $\delta J_X(\tau_1)$ at $I_X$ can be given therefore by

$$\delta J_X(\tau_1) = -\mu_{AX}(dA_X/dt) + \mu_X(dX/dt). \quad (60)$$

Since both disappearance rates of $A_X$ and $X$, $(-dA_X/dt)$ and $(-dX/dt)$, respectively, are given by $R_s$ in the steady state, Eq. 60 can be rewritten as

$$\delta J_X(\tau_1) = \{\mu_{AX} - \mu_X\}R_s. \quad (61)$$

(ii) The value of $J_X(\tau)$ during the residence time of $A_X$ may be given by

$$J_X(\tau) = -\{(d\mu/dt)N + 0\}_\tau;\ \tau_1 \leqq \tau \leqq \tau_2. \quad (62)$$

because $dN/dt = 0$ in this case. $N$ corresponds to $A_X$ and $A_X$ is constant during the time interval so that we have $dN/dt = 0$.

Considering Eq. 62, we have

$$\delta J_X(\tau_2) = -\{(d\mu_{AX}/dt)_{\tau=\tau 2} - (d\mu_{AX}/dt)_{\tau=\tau 1}\}A_X{}^{(s)} \quad (63)$$

where $-\{(d\mu_{AX}/dt)_{\tau=\tau 2} - (d\mu_{AX}/dt)_{\tau=\tau 1}\}$ corresponds to $w_{AX}{}^{(s)}$ introduced in Eq. 41, so that we have

$$\delta J_X(\tau_2) = w_{AX}{}^{(s)}A_X{}^{(s)}. \quad (64)$$

(iii) In the second step, $II_X$, according to a similar procedure to that for $I_X$, we have

$$\delta J_X(\tau_3) = \{\mu_{BX} - \mu_{AX}\}R_s. \quad (65)$$

(iv) In the second stage of $B_X$, according to a similar procedure to that for $A_X$, we have

$$\delta J_X(\tau_4) = w_{BX}{}^{(s)}B_X{}^{(s)}. \quad (66)$$

(v) In the last step, $III_X$, we have

$$\delta J_X(\tau_5) = \{\mu_{ZX} - \mu_{BX}\}R_s. \quad (67)$$

(3) On the other hand, $\{\delta J_X(\tau_n)\}$'s can be correlated with $\alpha_{IX}R_s$, $\alpha_{IIX}R_s$, and $\alpha_{IIIX}R_s$ as follows (see Fig. 10(b)):[22]

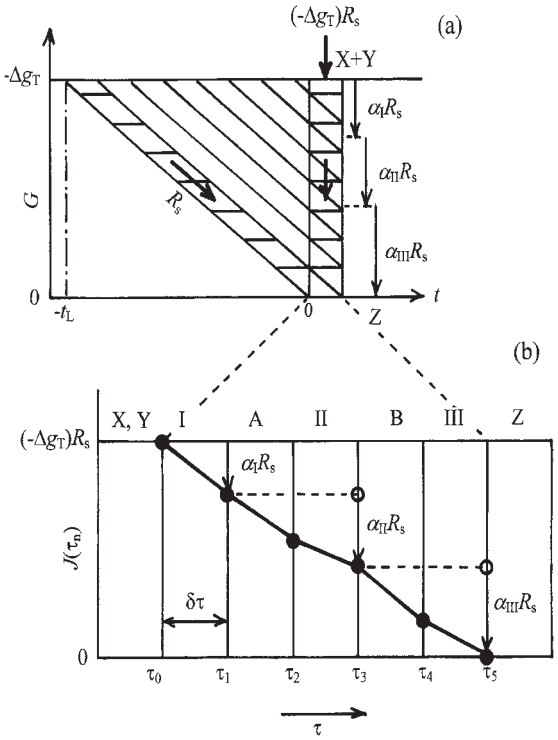


Fig. 10. (a) Gibbs free energy change with respect to X and Y versus real time $t$. The inclined line represents the change after the arrival on the surface of catalysts at $t = -t_L$ (elapsed time of the reaction). The vertical line at $t = 0$ represents the steady state. $R_s$: reaction rate at the steady state. $\alpha_I$, $\alpha_{II}$, and $\alpha_{III}$: affinities corresponding to those in Fig. 9. $-\Delta g_T$: Gibbs free energy drop of the reaction in Eq. 1. (b) Flows of the Gibbs free energy, $J(\tau_n)$, versus $\tau_n$ (see text).

$$\delta J_X(\tau_1) = -\alpha_{IX} R_s \quad (68)$$

$$\delta J_X(\tau_2) + \delta J_X(\tau_3) = -\alpha_{IIX} R_s \quad (69)$$

$$\delta J_X(\tau_4) + \delta J_X(\tau_5) = -\alpha_{IIIX} R_s. \quad (70)$$

Substituting the results of ($\alpha_{IX}$, $\alpha_{IIX}$, and $\alpha_{IIIX}$) given by Eqs. 50–52, and also $\delta J_X(\tau_2)$ and $\delta J_X(\tau_4)$ given by Eqs. 64 and 66, respectively, into Eqs. 68–70, we can derive expressions for $\delta J_X(\tau_1)$, $\delta J_X(\tau_3)$, and $\delta J_X(\tau_5)$ in terms of $l$. The results for all $\{\delta J_X(\tau_n)\}$ thus derived are summarized as:

$$\delta J_X(\tau_1) = -(l_{AX} l_{BX}/L_X) x(-\Delta g_T) R_s \quad (71)$$

$$\delta J_X(\tau_2) = -(l_{BX}/L_X) x(-\Delta g_T) R_s \quad (72)$$

$$\delta J_X(\tau_3) = -(l_{AX} l_{BX}/L_X) x(-\Delta g_T) R_s [= \delta J_X(\tau_1)] \quad (73)$$

$$\delta J_X(\tau_4) = -\{(1 + l_{AX})/L_X\} x(-\Delta g_T) R_s \quad (74)$$

$$\delta J_X(\tau_5) = -\{(1 + l_{AX}) l_{BX}/L_X\} x(-\Delta g_T) R_s. \quad (75)$$

The sum of Eqs. 71–75 leads to $-x(-\Delta g_T)R_s$ irrespective of $l$.

Integrating these $\delta J_X(\tau_m)$'s, we have

$$J_X(\tau_n) = (-\Delta g_T) R_s + \sum_{m=1}^{n} \delta J_X(\tau_m) \quad (76)$$

where $J_X(\tau_0)$ has been chosen as $(-\Delta g_T)R_s$, because it is convenient for comparing $J_X(\tau_n)$ with $J_Y(\tau_n)$ in Figs. 11–13.

(4) The results with respect to the Y-component can be easily derived from Eqs. 71–75 by replacing X for Y. For instance

$$\delta J_Y(\tau_1) = -(l_{AY} l_{BY}/L_Y) y(-\Delta g_T) R_s. \quad (77)$$

Integration of $\{\delta J_Y(\tau_m)\}$ leads to

$$J_Y(\tau_n) = (-\Delta g_T) R_s + \sum_{m=1}^{n} \delta J_Y(\tau_m) \quad (78)$$

where $J_Y(\tau_0)$ is chosen as $(-\Delta g_T)R_s$.[23]

(5) The sum of $J_X(\tau_n)$ and $J_Y(\tau_n)$ can be represented by

$$J_X(\tau_n) + J_Y(\tau_n) = (-\Delta g_T) R_s + \sum_{m=1}^{n} \{\delta J_X(\tau_m) + \delta J_Y(\tau_m)\} \quad (79)$$

where $\{J_X(\tau_0) + J_Y(\tau_0)\}$ may be given by $(-\Delta g_T)R_s$ according to the definition.

It should be emphasized that all relations derived in Section 4 have been described in terms of only $l$. Therefore, we can say that $k$ is concerned with the flow of materials, while $l$ is concerned with the flow of free energy.

## 5. Evaluation of $\delta J(\tau_n)$'s

**5.1 Determination of $x$ and $y$.** The values of $\delta J_X(\tau_1)$ $(= \delta J_X(\tau_3))$ determined by Eqs. 71 and 73 were positive, while those of $\delta J_Y(\tau_1)$ $(= \delta J_Y(\tau_3))$ were negative. Since $\delta J$ should be negative or zero for the step to proceed spontaneously, $\delta J_X(\tau_1)$ must be coupled with $\delta J_Y(\tau_1)$ or $\delta J_Y(\tau_3)$. It is assumed that[24]

$$\delta J_X(\tau_1) + \delta J_Y(\tau_1) = 0. \quad (80)$$

In the case of $\delta J_X(\tau_1) + \delta J_Y(\tau_1) < 0$, excess energy should be released at step I, which would inhibit the steady state (the case of a negative value at step III will be discussed below). The additional relation between $x$ and $y$ given by Eq. 80 leads to definite values of $x$ and $y$ because of $x + y = 1$. The results of $x$ and $y$ thus derived are given in Table 3.

**5.2 Evaluation of $\delta J_X(\tau_n)$ and $\delta J_Y(\tau_n)$.** Since we have

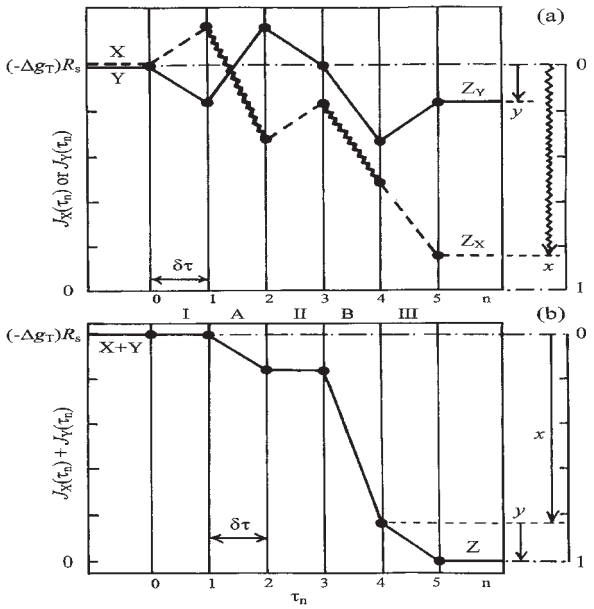


Fig. 11. (a) $J_X(\tau_n)$ and $J_Y(\tau_n)$ versus $\tau_n$ on Pt catalyst. (b) $J_X(\tau_n) + J_Y(\tau_n)$ versus $\tau_n$.

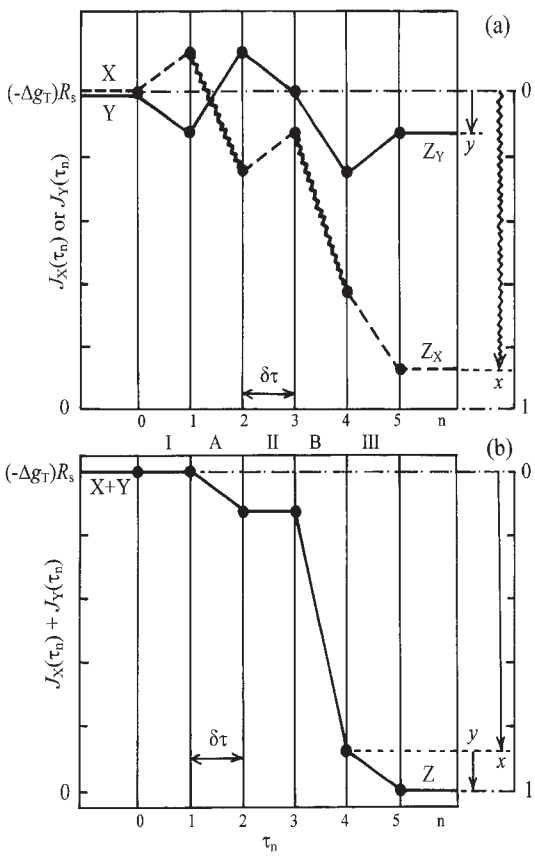


Fig. 12. (a) $J_X(\tau_n)$ and $J_Y(\tau_n)$ versus $\tau_n$ on Ru. (b) $J_X(\tau_n) + J_Y(\tau_n)$ versus $\tau_n$.

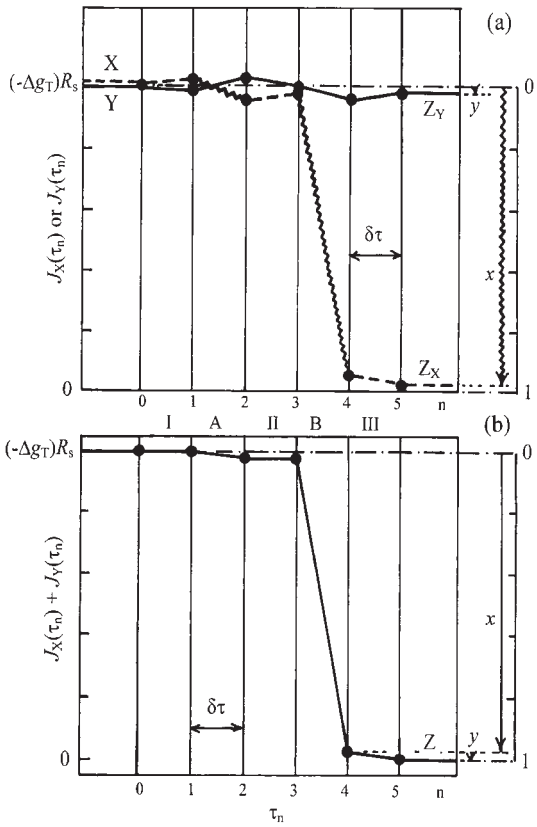


Fig. 13. (a) $J_X(\tau_n)$ and $J_Y(\tau_n)$ versus $\tau_n$ on Cu catalyst. (b) $J_X(\tau_n) + J_Y(\tau_n)$ versus $\tau_n$.

found the values of $x$ and $y$, the definite values of $\delta J_X(\tau_n)$ and $\delta J_Y(\tau_n)$ can be obtained from the parameters given in Table 2. The integrated results are illustrated in Figs. 11–13. It should be emphasized that although $J_X(\tau_n)$ and $J_Y(\tau_n)$ increased and/or decreased with increasing $\tau_n$, the sum of $\{J_X(\tau_n) + J_Y(\tau_n)\}$ decreased monotonically without any free energy barrier in agreement with the second law of thermodynamics. This result supports the assumption introduced in Eq. 80.

**5.3 Free Energy Dissipations.** (1) Substituting the results of $l_{AX} = -1/3$ obtained on Pt, Ru, and Cu into Eq. 56, we have the following relation:

$$A_X^{(s)} w_{AX}^{(s)} + B_X^{(s)} w_{BX}^{(s)} = -(1)x(-\Delta g_T)R_s \qquad (81)$$

irrespective of the values of $l_{BX}$. It is concluded therefore that the free energy drop of $x(-\Delta g_T)$ in the course of (i) in Fig. 1 is attributable to irreversible processes.[25]

(2) On the other hand, Eq. 56 applied to the Y-component leads to

$$A_Y^{(s)} w_{AY}^{(s)} + B_Y^{(s)} w_{BY}^{(s)} = -\{(1 + l_{AY} + l_{BY})/L_Y\} y(-\Delta g_T)R_s. \qquad (82)$$

Table 3. Values of $x$ and $y$

| Catal. | $x$ | $y$ |
|---|---|---|
| Pt | 0.841 | 0.158 |
| Ru | 0.876 | 0.124 |
| Cu | 0.979 | 0.021 |

Substituting the results of $l_{AY} + l_{BY} = -1$ obtained on Pt, Ru, and Cu, we have the result of

$$A_Y^{(s)} w_{AY}^{(s)} + B_Y^{(s)} w_{BY}^{(s)} = -(0)y(-\Delta g_T)R_s \qquad (83)$$

which means that no free energy dissipation is involved in the course of (ii) in Fig. 1.[26]

It is worth noting that since no free energy dissipation is involved in $\delta J_Y(\tau_n)$ changes, these values may be regarded *enthalpy*, so that $y(-\Delta g_T)R_s$ may be regarded as the "power [units: J/s or W]" produced out of the system in the course of the catalyzed reaction. Since $y$ depends on catalysts as shown in Table 3, the catalytic activity may be characterized by the power.

## 6. Discussion

**6.1 Elementary Reaction Rates.** (1) The flow of materials in the elementary reaction can be characterized by $k$.

Although $k_X$ and $k_Y$ in the first step are proportional to the amounts of catalysts, the other $k$ values are independent of the amounts of catalyst.[27] Since the units of all $k$ are $min^{-1}$, they can be compared with each other even if they were obtained on different catalysts and/or by different investigators.

(2) The ratio $k_{-AX}/k_{AX}$, for example, is rewritten as $(k_{-AX}\Delta A_X)/(k_{AX}\Delta A_X)$ and may be replaced by $\Delta S_{-IX}/\Delta S_{IIX}$ which denotes the ratio of the reverse reaction rate of the $A_X$-species to the forward one.[28] The ratios of $k_{-A}/k_A$ and $k_{-B}/k_B$ are summarized in Table 4.

(3) The negative value of $k_{-BY}$ means that the gradient $(dS_{-IIY}/dB_Y)$ was negative in the steady state, which means that the elementary reaction rate $S_{-IIY}$ in the step of $(1/2)O_2(a) \leftarrow O(a)$ decreases with increasing $B_Y$ $(= [O(a)])$.[19] The reverse reaction rate $S_{-IIY}$ determined by traditional methods was negligibly small.[29]

(4) The relaxation time of $\Delta A_X$ may be given by $(k_{-AX} + k_{AX})^{-1}$, because the disappearance rate of $\Delta A_X$ is given by $-(k_{-AX} + k_{AX})\Delta A_X$. On the other hand, if both elementary reaction rates of $S_{-IX}$ and $S_{IIX}$ are given by *linear functions* of $A_X$, the disappearance rate of $A_X$-*species* is expressed by $-(k_{-AX} + k_{AX})A_X$, and therefore the mean life time of $A_X$ is given by $(k_{-AX} + k_{AX})^{-1}$, which agrees with the relaxation time of $\Delta A_X$.

The relaxation times of $\Delta A$ and $\Delta B$ are summarized in Table 4.

(5) (i) The relaxation times of $\Delta A_X$ were longer than those

Table 4. Ratios of $k_{-A}/k_A$ and $k_{-B}/k_B$ and Relaxation Times (Units: s) of $(k_{-A} + k_A)^{-1}$ and $(k_{-B} + k_B)^{-1}$ Determined by the Results Given in Table 2

| Catal. | $k_{-AX}/k_{AX}$ | $(k_{-AX} + k_{AX})^{-1}$ | $k_{-BX}/k_{BX}$ | $(k_{-BX} + k_{BX})^{-1}$ | $k_{-AY}/k_{AY}$ | $(k_{-AY} + k_{AY})^{-1}$ |
|---|---|---|---|---|---|---|
| Pt | 1.82 | 1.38 | 3.62 | 0.16 | 2.64 | 37.9 |
| Ru | 0.41 | 1.81 | 3.67 | 0.36 | 0.83 | 26.9 |
| Cu | 0.23 | 0.36 | 1.19 | 0.02 | 0.11 | 13.6 |

of $\Delta B_X$ on every catalysts, as shown in Table 4. (ii) On the other hand, the relaxation times of $\Delta A_Y$ were longer than those of both $\Delta A_X$ and $\Delta B_X$ on every catalysts, as shown in Table 4. Because $k_{-BY} < 0$, the results of $(k_{-BY} + k_{BY})^{-1}$ are omitted.

(6) The results demonstrated in Figs. 6(b)–8(b) show that (i) $\Delta R(\omega)$ is affected mainly by $\Delta P_Y(\omega)$ on Pt. (ii) $\Delta R(\omega)$ is affected by both $\Delta P_X(\omega)$ and $\Delta P_Y(\omega)$ on Ru. (iii) $\Delta R(\omega)$ is affected mainly by $\Delta P_X(\omega)$ on Cu.

**6.2 Coupling among Elementary Reactions.** (1) The amplitude of coupling demonstrated in Figs. 11(a)–13(a) is evidently proportional to $y$. On the other hand, if $y = 0$ (then $x = 1$), the whole free energy drop $(-\Delta g_T)R_s$ of the reaction in Eq. 1 is dissipated during the reaction and would therefore correspond to a reaction without catalysts.

(2) The changes $\delta J_X(\tau_2)$ and $\delta J_X(\tau_4)$ are expected to be irreversible on the basis of Eq. 81 and are represented by the zigzag lines in Figs. 11(a)–13(a).

The driving force $\delta J_X(\tau_2)$ due to $A_X$ exceeded the barrier of $\delta J_Y(\tau_2)$ (>0) due to $A_Y$:

$$\delta J_X(\tau_2) + \delta J_Y(\tau_2) < 0. \tag{84}$$

The correlation could be interpreted by a model in which $A_Y$ migrated against a free energy gradient from strongly bound sites to weakly bound sites due to the driving force of $A_X$.[30]

(3) Compensation phenomena in heterogeneous catalysis have frequently been obserbed,[31] although they are questioned.[32] The phenomenon takes the form of a sympathetic linear correlation between the observed parameters of the Arrhenius equation $E_{app}$ and $\ln A_{app}$ for a series of related reactions or catalysts:

$$\ln A_{app} = mE_{app} + c. \tag{85}$$

The positive $\delta J_Y(\tau_2)$ is against the driving force of $\delta J_X(\tau_2)$, while the negative $\delta J_Y(\tau_4)$ accelerates the driving force stemming from $\delta J_X(\tau_4)$. (i) The hindrance of $\delta J_Y(\tau_2)$ to $\delta J_X(\tau_2)$ would be sensitive to reaction temperature, so that the coupling at $\tau_2$ could be assigned to the term corresponding to the activation energy $E_{app}$. (ii) The acceleration of $\delta J_Y(\tau_4)$ to $\delta J_X(\tau_4)$ could be assigned to the frequency factor expressed by $\ln A_{app}$ which does not depend on temperature.

The values of $y$ given in Table 3 depended on catalysts, so that $y$ could be regarded as the parameter[32] responsible for the compensation effects. The value of $y$ is shown in Fig. 14 as a function of $l_{BX}$ and $l_{BY}$ provided that $l_{AX} = -1/3$ and also $l_{AY} + l_{BY} = -1$. In the particular case of $l_{AY} = l_{BY} = -1/2$, we have $y < 1/6$ (in any case, $y < 0.286$).

(4) The changes stemming from $A_Y$ and $B_Y$, $\delta J_Y(\tau_2)$ and $\delta J_Y(\tau_4)$, are exactly compensated because of Eq. 83:

$$\delta J_Y(\tau_2) = -\delta J_Y(\tau_4). \tag{86}$$

This result might be interpreted by a model in which surface reconstruction occurred in the consecutive processes. The change without free energy dissipation may be regarded as a potential energy change.[33]

(5) In the last step producing $CO_2$ molecules, $\delta J_X(\tau_5)$ was negative, whereas $\delta J_Y(\tau_5)$ was positive, which led to

$$\delta J_X(\tau_5) + \delta J_Y(\tau_5) < 0. \tag{87}$$

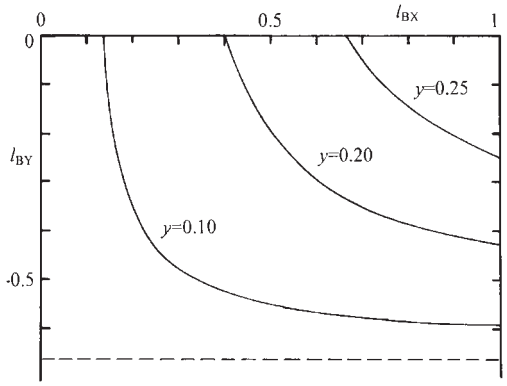


Fig. 14. The value of $y$ as a function of $l_{BX}$ and $l_{BY}$ provided that $l_{AX} = -1/3$ and $l_{AY} + l_{BY} = -1$.

Equation 87 suggests that (i) the motion of $CO(a_2)$ and O(a) must be coupled[34] for the reaction to occur spontaneously, and (ii) desorbing $CO_2$ molecules have excess energy.[35]

(6) The results of $J$ demonstrated in Figs. 11–13 are very different for many stand points from traditional potential energy profiles: (i) the ordinate is not energy but the flow of free energy, (ii) the free energy flow of both reactants X and Y are shown individually, (iii) the abscissa $\tau$ is defined rigorously by the elementary reaction steps, (iv) there is no transition state, chemical potentials of intermediate A and B are not constant but vary along the reaction coordinate.

(7) Every elementary reaction rate was affected more or less when one of the parameters in Table 2 was changed, which would deny a definite rate determining step.

**6.3 Microscopic Aspects.** (1) The complex rate coefficient $k_{AX}^*$, for example, can be rewritten as

$$(k_{AX} + i\omega l_{AX})\Delta A_X(t) = k_{AX}\Delta A_X(t) + l_{AX}\{dA_X(t)/dt\}. \tag{88}$$

On the other hand, according to Fick's second law of diffusion, the term of $\{dA_X(t)/dt\}$ in Eq. 88 can be correlated with the heterogeneity of $A_X$ on the surface:

$$\{\partial A_X(t)/\partial t\} = D_X\{\partial^2 A_X(t)/\partial r^2\}. \tag{89}$$

Therefore, spatiotemporal patterns of adsorbed species could be characterized by $l$ in the present RRS.

Surface diffusion has been considered in a kinetic model to explain the standing wave of spatiotemporal patterns in the CO oxidation on a Pt(110) surface. However, it seems difficult to derive reliable rate constants because of too many adjustable parameters.[36]

(2) The complex rate coefficient can be rewritten as

$$\begin{aligned}(k_{AX} + i\omega l_{AX})\Delta A_X(t) &\approx k_{AX}\Delta A_X{}^{(s)} \\ &\exp[i\omega\{t + (l_{AX}/k_{AX})\}](\omega \ll k_{AX}/l_{AX}) \\ &= k_{AX}\Delta A_X(t + (l_{AX}/k_{AX})).\end{aligned} \tag{90}$$

The *negative* values of $l_{AX}/k_{AX}$, $l_{AY}/k_{AY}$, and $l_{BY}/k_{BY}$ may be interpreted by each delay time at the elementary step, while the *positive* value of $l_{BX}/k_{BX}$ suggests that $\delta J_X(\tau_5)$ is a unique step in the reaction kinetics.

(3) Although dynamics of molecules can be observed by surface science techniques, the flow of free energy controlling the kinetics cannot be observed by traditional methods. Anoth-

er important merit of the present method for macro-kinetics would be in the investigation of *coupling* among elementary reactions.

**6.4 Modern Thermodynamics for Heterogeneous Catalysis.** (1) The transition state theory by Eyring[37] and Polanyi[38] has been applied to a heterogeneous catalytic reaction.[39] In basic transition state theory, the rate constant, $k$, is given by

$$k = (Q_{ts}/Q_{rs}) \exp(-E_a/RT) \tag{91}$$

under the assumption of quasi-equilibrium between the transition state and reactant state, which are described by the partition functions of $Q_{ts}$ and $Q_{rs}$, respectively. However, the intermediate A and B in this work differ from those in the transition state.

(2) According to the procedure to derive $dS_{univ}/dt$,[40] the second law of thermodynamics leads to

$$dS_{univ}/dt = \{-dG_{sys}/dt + \delta T(dS_{sys}/dt) - \delta P(dV_{sys}/dt) - dU_{mech}'/dt\}/T_{therm} \geq 0 \tag{92}$$

where $\delta T$ denotes the difference between the temperature of thermal surroundings, $T_{therm}$, and that of the system, $T_{sys}$. $\delta P$ denotes the difference between the pressure of the mechanical surroundings, $P_{mech}$, and that of the system, $P_{sys}$, which are defined as

$$T_{therm} \equiv T_{sys} + \delta T \text{ and } P_{mech} \equiv P_{sys} + \delta P \tag{93}$$

$U_{mech}'$ is the mechanical work without a change in the system volume, $V_{sys}$.

The rates of $dG_{sys}/dt$, $dS_{sys}/dt$, and $dV_{sys}/dt$ in Eq. 92 can be replaced by $(\Delta g_T)R_s$, $(\Delta s_T)R_s$, and $(\Delta v_T)R_s$, respectively, where $\Delta s_T$ and $\Delta v_T$ denote the entropy and volume changes in the reaction of Eq. 1, respectively. On the other hand, because $y(-\Delta g_T)R_s$ is power, as shown in section **5.3**, $dU_{mech}'/dt$ can be replaced by $y(-\Delta g_T)R_s$. Consequently, we have

$$dS_{univ}/dt = \{x(-\Delta g_T) + \delta T(\Delta s_T) - \delta P(\Delta v_T)\}R_s/T_{therm} \geq 0 \tag{94}$$

where $x + y = 1$ has been considered. The terms of $\delta T(\Delta s_T)$ and $-\delta P(\Delta v_T)$ are usually positive.

It is worth noting that (i) Eq. 94 means that the heat of reaction can be given by $\{(-\Delta h_T) - y(-\Delta g_T)\}R_s$ and therefore it would depend on catalysts, where $\Delta h_T$ denotes the enthalpy change in the reaction of Eq. 1. (ii) In a reversible process, $x$, $\delta T$, and $\delta P$ are zero, so that we have $dS_{univ}/dt = 0$.

(3) The most general form of the second law of thermodynamics is expressed by[3]

$$d_iS \geq 0 \text{ or } d_iS/dt \geq 0 \tag{95}$$

where $d_iS$ means the entropy change due to "uncompensated transformation", the entropy produced by the irreversible processes in the *interior* of the system.

However, $\delta J$ is proportional to $-dG_{sys}/dt$ and therefore not $d_iS/dt$, but $dS_{univ}/dt$, is profitable to interpret $\delta J$.

(4) The activity of catalysts has been shown to be characterized by the power of $y(-\Delta g_T)R_s$. It seems of interest that the situation is the same as a gasoline engine, because it produces power in the course of combustion. The situation may be generalized further to a living thing. Consequently, the quantitative investigation of a catalyzed reaction can contribute to the development of modern thermodynamics.

## 7. Conclusion

(1) In studying the kinetic nature of catalysis, (i) $dG/dt$ instead of $G$ is essential so as to be discussed in modern thermodynamics,[3] (ii) $d(\mu N)/dt$ is more fruitful than $dG/dt$ in the theoretical treatment, and (iii) $dS_{univ}/dt$ is more fundamental than $d_iS/dt$.

(2) The novel state functions of $\tau$, $J_X(\tau)$, and $J_Y(\tau)$ have been derived, which reveal that (i) elementary processes involved in the reaction mechanism must be coupled with each other, (ii) no transition state exists in the course of the overall reaction, and (iii) the kinetic parameters evaluated appear to be consistent in many cases with results obtained by surface science techniques.

(3) The semi-empirical results of $l_{AX} = -1/3$ and $l_{AY} + l_{BY} = -1$ reveal that CO(X) plays an active role, while $O_2$ plays a passive role in the reaction, although they are coupled. The power produced in the course of the reaction is given by $y(-\Delta g_T)R_s$.

(4) Although the present results evidently leave room for more accurate investigation and extension to other experimental conditions, it is concluded that (i) the novel rate coefficient $l$ plays an essential role in studying the flow of free energies, (ii) in order to determine $l$, the *harmonic* perturbation for reactants is indispensable, and (iii) the scan of the frequency of the perturbation over a wider range is preferable to determine reliable kinetic parameters.

Consequently, the present method may be named "reaction rate spectroscopy"[41] and can contribute to quantitative studies of the complex phenomenon of catalysis.

I (Y. Y.) wish to thank Dr. Kazunori Tanaka (Nihon University) for his fruitful discussions about the kinetics in heterogeneous catalytic reactions and Dr. Fujito Nemoto (Osaka Institute of Technology) for his valuable discussions about modern thermodynamics in heterogeneous catalysis.

## References

1 M. M. Slin'ko and N. I. Jaeger, "Oscillating Heterogeneous Catalytic Systems," Studies in Surface Science and Catalysis, Vol. 86, Elsevier, Amsterdam (1994).

2 R. Imbihl and G. Ertl, *Chem. Rev.*, **95**, 697 (1995).

3 D. Kondepudi and I. Prigogine, "Modern Thermodynamics," Wiley, Chichester (1998).

4 S. W. Weller, *Catal. Rev.-Sci. Eng.*, **34**, 227 (1992).

5 C. O. Bennett, *Adv. Catal.*, **44**, 329 (1999).

6 M. Pekar and J. Koubek, *Appl. Catal., A*, **177**, 69 (1999).

7 Y. Yasuda, *J. Phys. Chem.*, **93**, 7185 (1989).

8 J. R. Schrieffer and J. H. Sinfelt, *J. Phys. Chem.*, **94**, 1047 (1990).

9 Contrary to the expectation, the amplitude became higher in a reaction system at a steady state as shown below.

10 Y. Yasuda, *Heterog. Chem. Rev.*, **1**, 103 (1994).

11 S. C. Reyes and E. Iglesia, "Catalysis," Royal Society of Chemistry (1994), Vol. 11, Chap. 2.

12 Y. Yasuda, K. Iwai, and K. Takakura, *J. Phys. Chem.*, **99**, 17852 (1995).

13 Y. Yasuda and Y. Kuno, *J. Phys. Chem. A*, **102**, 4878 (1998).

14 Y. Yasuda and Y. Kuno, *J. Phys. Chem. B*, **103**, 3916 (1999).

15 Y. Yasuda, H. Mizusawa, and T. Kamimura, *J. Phys. Chem. B*, **106**, 6706 (2002).

16 T. Engel and G. Ertl, *Adv. Catal.*, **28**, 1 (1976).

17 The $A_X$- and $B_X$-species were not distinguished in a previous paper.[15] The two-step model was modified to the three-step model in this work, because the two-step model was not effective to reproduce every result obtained by the three kinds of catalysts adopted.

18 Although the rate coefficient $k_Z$ corresponding to the reverse reaction at step III was considered in the numerical simulation, $k_Z \fallingdotseq 0$ was derived.

19 Since the perturbation caused by $\Delta V(t)$ was very small ($v \approx 10^{-2}$), any non-linear rate equation can be linearized by a Taylor series expansion around a steady state, neglecting the second order term in the expansion. For example, the appearance rate $R$ of $CO_2$(g) at step III may be expressed by

$$R(B_X(t), B_Y(t)) = R(B_X^{(s)}, B_Y^{(s)}) + k_{BX}{}^* \Delta B_X(t) + k_{BY}{}^* \Delta B_Y(t) \quad \text{(A1)}$$

where the short notation is introduced: $k_{BX} \equiv (\partial R/\partial B_X)^{(s)}$ and $k_{BY} \equiv (\partial R/\partial B_Y)^{(s)}$.

Although only the first term $R(B_X^{(s)}, B_Y^{(s)})$ $(= R_s)$ has usually been discussed in a traditional method [for example, M. Boudart and K. Tamaru, *Catal. Lett.*, **9**, 15 (1991)], the variation $\Delta R$ given by $k_{BX}{}^* \Delta B_X(t)$ and $k_{BY}{}^* \Delta B_Y(t)$ is considered in this work besides $R_s$.

20 The result of $k_{-BY}$ being negative means that $k_{BY} \equiv (\partial S_{-IIY}/\partial B_Y)^{(s)} < 0$.

21 At step $II_X$, for example, both disappearance of $A_X$ and appearance of $B_X$ (represented by $A_X \rightarrow B_X$) occur at the same time. However, they are separated by $\delta\tau$ in abscissa of the reaction coordinate. If the upper limit $\tau_5$ is normalized as unity (i.e., $0 \leqq \tau_n \leqq 1$), the value of $\delta\tau$ becomes 1/5.

22 Identical change is represented in different ways in each equation of Eqs. 68–70: (i) in Eq. 68 both sides represent the free energy drop when X disappears and $A_X$ appears; (ii) in Eq. 69 both sides represent the drop when $A_X$ disappears and $B_X$ appears; (iii) in Eq. 70 both sides represent the drop when $B_X$ disappears and $Z_X$ appears.

23 The identical integration constant for X and Y was chosen in order to compare $\delta J_X$ with $\delta J_Y$.

24 Because $\delta J_Y(\tau_4) < 0$, the other combination of $\delta J_X(\tau_1) + \delta J_Y(\tau_4)$ would be possible. However, it is not acceptable, because $\delta J_X(\tau_1)$ occurs instantaneously whereas $\delta J_Y(\tau_4)$ covers the mean life time of the $B_Y$-species.

On the other hand, if another choice of

$$\delta J_X(\tau_2) + \delta J_Y(\tau_2) = 0 \quad \text{(A2)}$$

is adopted, the values of $x$ and $y$ derived from the restriction of Eq. A2 leads to

$$\delta J_X(\tau_1) + \delta J_Y(\tau_1) > 0 \quad \text{(A3)}$$

which also is not acceptable.

25 The results of $-1/3$ for $l_{AX}$ on every catalyst were determined semi-empirically. Because they were very close to $-1/3$ in repeated numerical simulations, they were assumed to be $-1/3$.

26 The results of $l_{AY} + l_{BY} = -1$ on every catalyst were determined semi-empirically. Because they were very close to $-1$ in repeated numerical simulations, they were assumed to be $-1$.

27 For example, both $dZ(t)/dt$ and $\Delta B_X(t)$ or $\Delta B_Y(t)$ in Eq. 24 depend on the amount of catalysts and therefore the coefficient $k_{BX}{}^*$ and $k_{BY}{}^*$ should be independent of it.

28 On the other hand, the ratio of $\Delta S_{-IIX}/\Delta S_{IIX}$ at step $II_X$, for example, can be rewritten as $k_{-BX}\Delta B_X(t)/k_{AX}\Delta A_X(t)$. Because $\Delta B_X(t)$ and $\Delta A_X(t)$ are expressed by Eqs. 13 and 11, respectively, it is possible to describe explicitly the value of $\Delta S_{-IIX}/\Delta S_{IIX}$ but the result depends on $\omega$ as well as all (sixteen) rate coefficients. The result is very complicated. However, the ratio of $\Delta S_{-IX}/\Delta S_{IIX}$ can be expressed by $k_{-AX}/k_{AX}$. The simple result is necessarily independent of $\omega$ and constant.

29 T. Engel and G. Ertl, "The Chemical Physics of Solid Surfaces and Heterogeneous Catalysis," D. A. King, D. P. Woodruff, Elsevier, Amsterdam (1982), Vol. 4, Chap. 3.

30 It is found that surface species may migrate not only from weakly bound sites to strongly bound sites (enthalpy favorable process) but also from strongly bound sites to weakly bound sites (enthalpy unfavorable process) during heterogeneous catalysis reactions [W. X. Huang, X. H. Bao, H. H. Rotermund, and G. Ertl, *J. Phys. Chem. B*, **106**, 5645 (2002)].

31 G. C. Bond, "Catalysis by Metals," Academic Press, London (1962).

32 G. C. Bond and M. A. Keane, *Catal. Rev.-Sci. Eng.*, **42**, 323 (2000).

33 An adsorbate induced surface reconstruction is proposed as a possible driving force for oxide formation on Pt(100) during CO oxidation [J. Dicke, H. H. Rotermund, and J. Lauterbach, *Surf. Sci.*, **454–456**, 352 (2000)].

34 Formation of $CO_2$ with neighboring surface oxygen atoms (called O-bridge) has been observed [J. Wang, C. Y. Fan, K. Jacobi, and G. Ertl, *Surf. Sci.*, **481**, 113 (2001)]; it is found further that the formation of the surface oxide has a dramatic effect on the $CO_2$ production rate on Pt(110) [B. L. M. Hendriksen and J. W. M. Frenken, *Phys. Rev. Lett.*, **89**, 046101 (2002)].

35 (i) $CO_2$ molecules produced by the oxidation of CO on Pt has been vibrationaly excited [K. Kunimori, K. Watanabe, H. Ohnuma, and H. Uetsuka, *Surf. Sci.*, **368**, 366 (1996)]. (ii) The angular and velocity distributions of desorbing product $CO_2$ were studied in a steady-state CO oxidation on Pt(110) at around 500 K, while the translational temperature reached about 1820 K [M. G. Moula, A. B. P. Mishra, I. Rzeznicka, M. U. Kislyuk, S. Liu, Y. Ohno, and T. Matsushima, *Chem. Phys. Lett.*, **341**, 225 (2001)]. These hyperthermal energies are discussed [E. Molinari and M. Tomellini, *Chem. Phys.*, **277**, 373 (2000)]. The excess energy of $y(-\Delta g_T)$ was ca. 40 kJ/mol on Pt and consistent with the excess energy observed.

36 A. Oertzen, H. H. Rotermund, A. S. Mikhailov, and G. Ertl, *J. Phys. Chem. B*, **104**, 3155 (2000).

37 H. Eyring, *J. Chem. Phys.*, **3**, 107 (1935).

38 M. G. Evans and M. Polanyi, *Trans. Faraday Soc.*, **31**, 875 (1935).

39 J. Horiuti, *J. Res. Inst. Catal., Hokkaido Univ.*, **5**, 1 (1957).

40 $dU_{mech} = P_{mech}dV_{sys} + dU_{mech}'$; $dU_{therm} = -(dH_{sys} + dV_{sys}\delta P + dU_{mech}')$; $dS_{therm} = dU_{therm}/T_{therm}$; $dS_{univ} = dS_{therm} + dS_{sys}$. [G. M. Barrow, "Physical Chemistry, 6th ed," McGraw, Boston (1996)].

41 A dynamic method for characterization of adsorptive properties of solid catalysts was named "adsorption-rate spectrum" [L. Polinski and L. Naphtali, *Adv. Catal.*, **19**, 241 (1969)]. Relaxation

techniques such as acoustic wave and alternating electric field was suggested by Eigen to be named "relaxation spectroscopy".[4] The present method based on $\delta J$ may be named "reaction-rate spectroscopy", because the novel method would play an important role in modern thermodynamics.